Crystal structure, electric and magnetic properties in Na_xCoO_2

K.Nagasawa and H.Nakatsugawa

Division of Materials Science and Engineering, Graduate School of Engineering, Yokohama National University

79-5 Tokiwadai, Hodogaya Ward, Yokohama 240-8501 Japan

E-mail: naka@ynu.ac.jp, Phone: +81-45-339-3854, Fax: +81-45-331-6593

Abstract

The electron density distributions of -Na_xCoO_2 have been obtained by the maximum entropy method and the Rietveld analysis using powder x-ray diffraction data at room temperature. In the Rietveld refinement, the deviation of (008) and (108) peaks is very large relative to that of other reflections, and the change in x-ray diffraction data is clearer than that in neutron diffraction data at 10K and room temperature. This indicates that electron density distributions in -Na_xCoO_2 are slightly modulated with increasing x. In fact, there found to be the obvious overlapping of the charge density between O O network and Co ions, but no significant overlapping with increasing x. This is the direct observation of decrease of covalency between O $2p$ and Co t_{2g} in the CoO_2 layer with increasing the sodium content.

Introduction

Recently, a layered cobalt oxide Na_xCoO_2 have been known as a promising candidate for thermoelectric materials because of its large thermoelectric power (S) coexisting with low electric resistivity ( ).[1] The carrier concentration has been found to be much higher in this system, i.e., the order of 10^{21} 10^{22} cm^{-3}, than in some known thermoelectric materials such as Bi_2Te_3 and PbTe.[2] The large value reported for S of $Na_{0.5}CoO_2$, i.e., S >50μ V/K at room temperature, is difficult to be understood within the framework of conventional one-electron picture.[3] A recent result of heat capacity measurements [4] revealed that the effective mass of the carrier (holes) of this compound was as large as those of strongly correlated electrons. Terasaki [3] suggested that both the strong electron correlation and the spin sate in Co site play a crucially important role in the enhancement of S. The magnetic susceptibility ( ) of polycrystalline sample of $Na_{0.5}CoO_2$ was successfully explained by the coexistence of Co^{3+} (low-spin: t_{2g}^6) and Co^{4+} (low-spin: t_{2g}^5). [5] Koshibae et al. [6] established a theory generalizing the Heikes' formula [7] and suggested that the observed large magnitude of S in Na_xCoO_2 would be originated from both the large degeneracy of Co species of various spin states and the strong correlation of $3d$ electrons. It was concluded that the low-spin state in Co site is a key factor for the large Seebeck coefficient.

The structure of the material is of a layer type consisting of CdI_2-type CoO_2 conducting layers which are made of edge-shared CoO_6 octahedra and interlayers of Na^+ ions alternately stacked along the c-axis. The sodium ions are intercalated in trigonal prismatic or octahedral coordination of oxygen atoms and are mobile even at room temperature, but the ionic conductivity is much smaller than the electronic conductivity in the CoO_2 layers. Delmas et al. [8] have reported that Na_xCoO_2 has four distinct bronze-type phases, i.e., (O3-

type structure), '(O'3-type structure), (P3-type structure), and (P2-type structure), and the difference among these four phases is in the stacking sequence of oxygen atom layers. The neutron diffraction investigation [9] of $Na_{0.74}CoO_2$ has shown that the material has a hexagonal phase (space group: $P6_3/mmc$, No.194) and that there are two types of Na^+ sites, i.e., $2b$ (0, 0, 1/4) and $2d$ (2/3, 1/3, 1/4), with different occupancies. The $2d$ site is in a trigonal prismatic environment, while the $2b$ site has neighboring Co ions above and below the trigonal prism of the oxygen atom, which should cause the difference in the occupancy. Such a disordered structure also should cause a low thermal conductivity, i.e., 20mW/cmK at room temperature, which was attributed to the short phonon mean free path arising from the Na deficiency. [10]

Na_xCoO_2 is known to show a wide range of Na nonstoichiometry within 0.5 x 1.0, where the valence of Co changes $Co^{3+}_xCo^{4+}_{1-x}$ in accordance with Na^+ content x. Since Na is volatile, it has been recognized that the control of x is difficult for Na_xCoO_2 by a conventional solid state reaction method. [11] Recently, however, Motohashi et al. [12,13] established an unconventional method named rapid heat-up (RH) technique to precisely control the sodium content in Na_xCoO_2 samples, in which Na evaporation during the synthesis is minimized. For thus prepared samples of $Na_{0.75}CoO_2$ exhibit S 120μ V/K at room temperature, [12] and show a magnetic transition of the second order below 22K. [13] These features strongly indicate the appearance of an unusual electronic state that may be attributed to strongly correlated electrons in $Na_{0.75}CoO_2$. Furthermore, Tojo et al. [14] measured the heat capacity of $Na_{0.75}CoO_2$ and found first order phase transitions at 288.7, 296.3, and 302.1K. The x-ray diffraction patterns in $Na_{0.75}CoO_2$ at 123 and 333K indicate that the most probable mechanism of the phase transition around room temperature is the occurrence of some kind of ordering in Na^+ layers. [14] Although a large number of studies have been made on the strongly correlated electron system in the CoO_2 layers, little is known about a relationship between the CoO_2 layers and the Na^+ layers. Thus, a further investigation is needed to confirm these clearly. From this point of view, the magnetic properties, the parameters of the crystal structure, and the charge density distributions visualized by a combination of the maximum entropy method (MEM) and a Rietveld refinement [15,16] in Na-richer samples by a conventional solid state reaction method have been investigated in the present study.

Experimental procedure

Four polycrystalline Na-richer samples of -Na_xCoO_2 were prepared by the RH technique [12,13] to precisely control the sodium content. Starting powders of Na_2CO_3 and

Co_3O_4 were mixed and calcined at 1153K for 12h in air. Then, the samples were reground, pressed into pellets and sintered at 1193K for 12h in air. Finally, the pellets were cooled in the furnace to room temperature at a rate of 1K/min. The resulting powder sample was characterized by x-ray diffraction (XRD), neutron diffraction (ND) and inductively coupled plasma atomic-emission spectrometry (ICP-AES) analysis. The XRD and ND patterns showed good identification of the samples as the phase, and there was no indication of the presence of other prototypes or residual raw materials. The molar ratio of metal ions in the samples for -Na_xCoO_2 was determined to be Na : Co = (i) 0.77(6) : 1 , (ii) 0.78(3) : 1 , (iii) 0.79(9) : 1, and (iv) 0.82(6) : 1 by the ICP-AES analysis.

The XRD measurement was carried out using a JEOL JDX-3530 x-ray diffractometer system at room temperature. The powder sample is pressed on a glass plate, mounted vertically on the sample table and diffraction patterns are recorded using CuKα (=1.54) radiation. The XRD data is collected in 2theta range from 10 to 90° in steps of 0.02° using a scintillation detector. We performed powder ND experiments at 10 and 300K on the Kinken powder diffractometer for high efficiency and high resolution measurements, HERMES, of Institute for Materials Research (IMR), Tohoku University, installed at the JRR-3M reactor in Japan Atomic Energy Research Institute (JAERI), Tokai Establishment. [17] An incident neutron wavelength =1.82035(7) was obtained from a Ge(311) monochromater. The fine powder sample was sealed in a vanadium cylinder with helium gas, and mounted at the cold head of a closed cycle He-gas refrigerator. The ND data were collected on thoroughly ground powders by a multi-scanning mode in the 2theta range from 10° to 153° with a step width of 0.10°.

The structure determination of -Na_xCoO_2 was analyzed using the Rietveld analysis program, RIETAN-2000. [18] The charge density distributions at room temperature were visualized by an elaborate method, which are combination of the MEM and the Rietveld refinement of the XRD data. [15,16] Moreover, magnetic susceptibility ( ) was measured between 10 and 300 K using a commercial apparatus from Quantum Design MPMS superconducting quantum interference device (SQUID) magnetometer.

Results and discussion

The powder XRD data showed that the samples for x=0.77(6), 0.78(3), 0.79(9), and 0.82(6) were single phase and had the P2-type hexagonal structure at room temperature, where the highest symmetry $P6_3/mmc$ type space group (No.194) was chosen as it described the refined structure equally. [9] In Figs.1(a) and 1(b), the results of the Rietveld refinement are shown for (a) x=0.77(6) and (b) x=0.79(9). In the present analysis we assumed that Na1 and Na2 ions occupy *2b* (0,0,1/4) and *2d* (2/3,1/3,1/4) sites, respectively. The weighted profile reliability factors of the Rietveld refinement as a pre-analysis for the MEM, R_{wp}, were (a) 15.01% and (b) 16.77%. The reliability factors based on the integrated intensities, R_I, were (a) 2.97% and (b) 6.61%. There are good agreement between the results of the Rietveld

refinement, except for two peaks, i.e., (008) (2theta 68° 69°) and (108) (2theta 80° 81°). It should be noted that (112) and (202) reflections deviate to low 2theta angle side, but (008) and (108) reflections deviate to high 2theta angle side with increasing x.

(a)
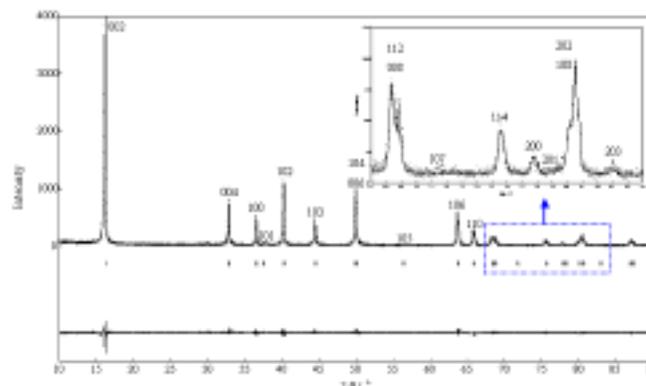
(b)
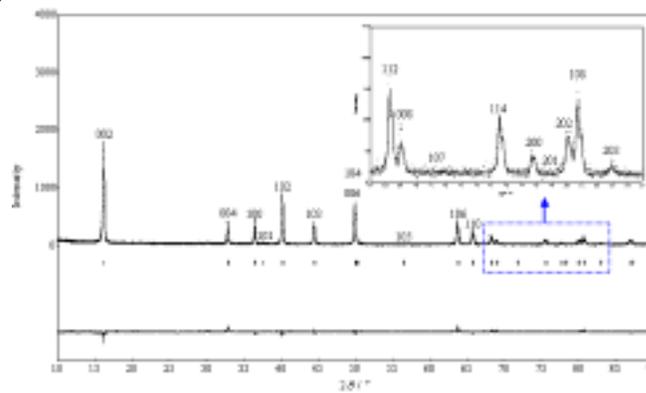
Figure 1: Rietveld fitting of XRD data for (a) x=0.77(6) and (b) x=0.79(9) at room temperature.

The powder ND data also showed that the specimens for x=0.77(6), 0.78(3), 0.79(9), and 0.82(6) had the P2-type hexagonal structure which was assigned to $P6_3/mmc$ (No.194) at 10K and room temperature. In Figs.2(a) and 2(b), the results of the Rietveld refinement at 10K are shown for (a) x=0.77(6) and (b) x=0.79(9). No impurity peak was detected in the present powder ND measurements. The weighted profile reliability factors of the Rietveld refinement, R_{wp}, were (a) 7.66% and (b) 7.15%. The reliability factors based on the integrated intensities, R_I, were (a) 6.43% and (b) 7.13%. There are two kinds of prisms, i.e., $Na1O_6$ and $Na2O_6$ prisms. [19] The $Na1O_6$ prism at *2b* site shares two sets of three oxygen atoms with upper and lower one CoO_6 octahedara, respectively. On the other hand, the $Na2O_6$ prism at *2d* site shares two sets of three oxygen atoms with upper and lower three CoO_6 octahedara, respectively. Judging from the ionic radius of Na^+ for six coordinations (1.02), [20] the Na^+ ions cannot fully occupy the adjacent *2b* and *2d* sites because of the Na1-Na2 distances. Thus, the sodium ions are randomly distributed at the *2b* and *2d* sites with different occupancies. Sodium content was determined to be 0.776 (*2b*:0.255 + *2d*:0.521) for -$Na_{0.78}CoO_2$ and 0.799 (*2b*:0.265 + *2d*:0.534)

for $-Na_{0.80}CoO_2$ which are in good agreement with that obtained by the ICP-AES chemical analysis.

(a)

(b)
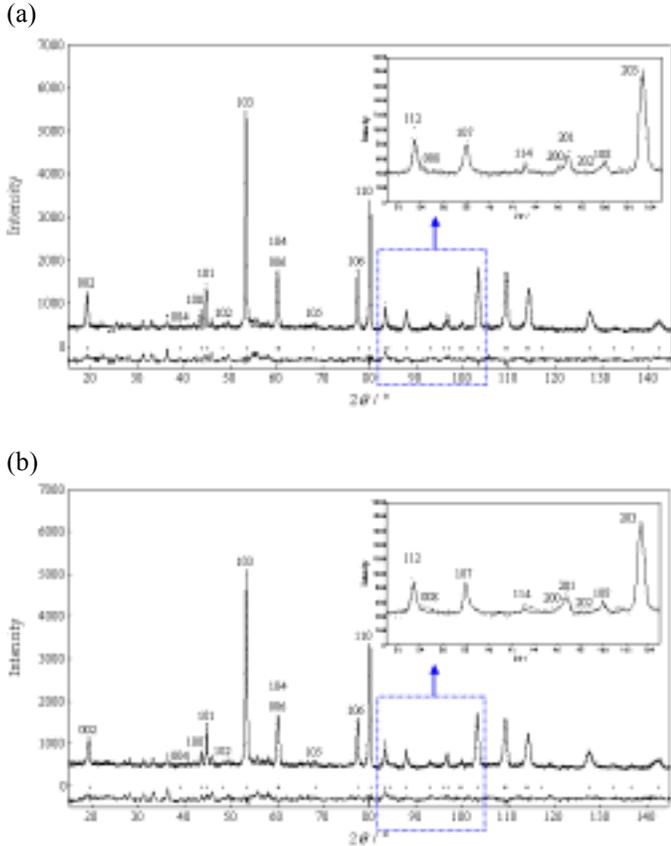
Figure 2: Rietveld fitting of ND data for (a) x=0.77(6) and (b) x=0.79(9) at 10K.

The number of observed XRD structure factors derived in the Rietveld analysis at room temperature were 24 for each set of data, which were used for further MEM analysis. Following the Rietveld analysis, the MEM analysis was carried out with a computer program, MEED, [21] using 32× 32× 32 pixels. In the MEM imaging, any kind of deformation of electron densities is allowed as long as it satisfies the symmetry requirements. This method enables us to visualize more detailed features included in the observed data like the bonding electron distribution associated with hybridized orbitals.

In Figs.3(a) and 3(b), the three-dimensional representation of the MEM charge densities for samples of (a) x=0.77(6) and (b) x=0.79(9) together with the MEM charge densities in the (002) plane for both samples. An equi-contour surface is drawn only for the lower density region. In these figures, there are O O network of the electron density due to the $O2p - O2p$ orbital hybridization. There found to be an obvious overlapping of the charge density between O O network and Co for x=0.77(6), but no significant overlapping for x=0.79(9). This is the direct observation of decrease of the Co O hybridization in the CoO_2 layer with increasing the sodium content from x=0.77(6) to 0.82(6). In particular, the change in the electron density distribution should be attributed to the increase of the lattice parameter a and the Co O distance with increasing x.

(a)

(b)
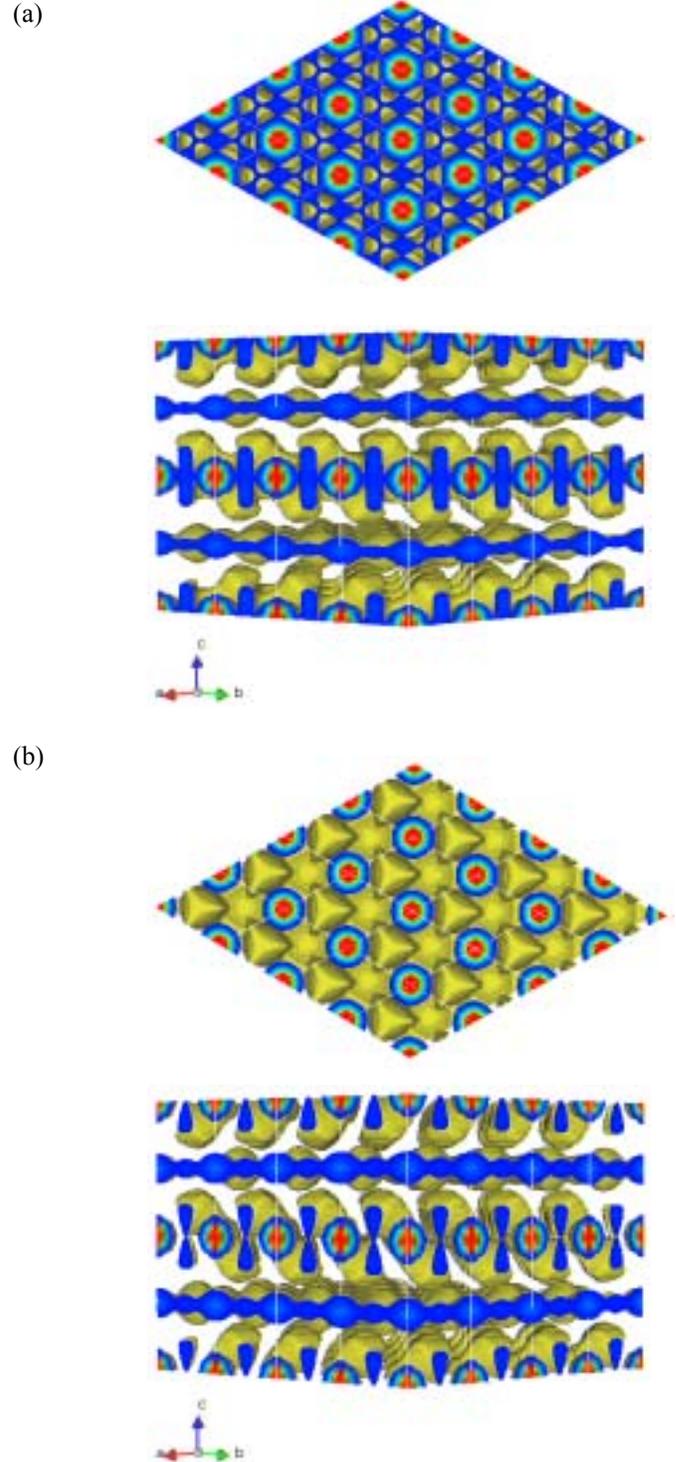
Figure 3: Three-dimensional representation of the MEM charge distribution at room temperature for (a) x=0.77(6) and (b) x=0.79(9).

Conclusion

The samples of $-Na_{0.78}CoO_2$ and $-Na_{0.80}CoO_2$ were single phase and had the P2-type hexagonal structure (space group: $P6_3/mmc$, No.194) at 10K and room temperature. In

the present analysis we assumed that Na1 and Na2 ions occupy *2b* and *2d* sites, respectively. The sodium ions cannot fully occupy the adjacent *2b* and *2d* sites so that these are randomly distributed at the both sites with different occupancies. In the Rietveld refinement, there are good agreement between x=0.77(6) and x=0.79(9), except for (008) and (108) peaks. The deviation of the two reflections is very large relative to that of other reflections, and the change in XRD data is clearer than that in ND data. This means that electron density distributions in -Na_xCoO_2 are slightly modulated with increasing x. In fact, there found to be the obvious overlapping of the charge density between O O network and Co ions for x=0.77(6), but no significant overlapping for x=0.79(9). This is the direct observation of decrease of the Co O hybridization in the CoO_2 layer with increasing the sodium content.

Acknowledgments

References

1. Terasaki, I., Sasago, Y., and Uchinokura K., "Large thermoelectric power in $NaCo_2O_4$ single crystals" Phys.Rev B Vol. 56, pp. R12685-R12687 (1997).

2. Mahan G., Sales B., and Sharp J., "Thermoelectric materials: new approaches to an old problem" Phys.Today Vol. 50, pp. 42-47 (1997).

3. Terasaki I., *in Proceedings of the 18th International Conference on Thermoelectrics* (ICT1999), Baltimore, MD, Aug.29-Sept.2, 1999 (IEEE, Piscataway, 2000), pp. 569-576.

4. Ando Y., Miyamoto N., Segawa K., Kawata T., and Terasaki I., "Specific-heat evidence for strong electron correlations in the thermoelectric material $(Na,Ca)Co_2O_4$" Phys.Rev. B Vol. 60, pp. 10580-10583 (1999).

5. Ray R., Goshray A., Goshray K., and Nakamura S., "[59]Co NMR studies of metallic $NaCo_2O_4$" Phys.Rev. B Vol. 59, pp. 9454-9461 (1999).

6. Koshibae W., Tsutsui K., and Maekawa S., "Thermopower in cobalt oxides" Phys.Rev. B Vol. 62, pp. 6869-6872 (2000).

7. Heikes R. R. and Ure R. W., Jr., Thermoelectricity: Science and Engineering (Interscience, New York, 1961).

8. Delmas C., Braconnier J-. J., Fouassier C., and Hagenmuller P., "Electrochemical intercalation of sodium in Na_xCoO_2 bronzes" Solid State Ionics Vol. 3-4, pp. 165-169 (1981).

9. Balsys R. J. and Davis R. L., "Refinement of the structure of $Na_{0.74}CoO_2$ using neutron powder diffraction" Solid State Ionics Vol. 93, pp. 279-282 (1996).

10. Takahata K., Iguchi Y., Tanaka D., Itoh T., and Terasaki I., "Low thermal conductivity of the layered oxide $(Na,Ca)Co_2O_4$: Another example of a phonon glass and an electron crystal" Phys.Rev. B Vol. 61, pp. 12551-12555 (2000).

11. T.Kawata, Y.Iguchi, T.Itoh, K.Takahata, and I.Terasaki, "Na-site substitution effects on the thermoelectric properties of $NaCo_2O_4$" Phys.Rev. B Vol. 60, pp. 10584-10587 (1999).

12. Motohashi T., Naujalis E., Ueda R., Isawa K., Karppinen M., and Yamauchi H., "Simultaneously enhanced thermoelectric power and reduced resistivity of $Na_xCo_2O_4$ by controlling Na nonstoichiometry" Appl.Phys.Lett. Vol. 79, pp. 1480-1482 (2001).

13. Motohashi T., Ueda R., Naujalis E., Tojo T., Terasaki I., Atake T., Karppinen M., and Yamauchi H., "Unconventional magnetic transition and transport behavior in $Na_{0.75}CoO_2$" Phys.Rev. B Vol. 67, pp. 064406-1-064406-5 (2003).

14. Tojo T., Kawaji H., and Atake T., "First-order phase transition in $Na_{1.5}Co_2O_4$" Phys.Rev. B Vol. 65, pp. 0521105-1-0521105-3 (2002).

15. Takata M., Umeda B., Nishibori E., Sakata M., Saito Y., Ohno M., and Shinohara H., "Confirmation by X-ray diffraction of the endohedral nature of the metallofullerene $Y@C_{82}$" Nature Vol. 377, pp. 46-49 (1995).

16. Takata M., Nishibori E., Umeda B., Sakata M., Yamamoto E., and Shinohara H., "Structure of endohedral dimetallofullerene $Sc_2@C_{84}$" Phys.Rev.Lett. Vol. 78, pp. 3330-3333 (1997).

17. Ohoyama K., Kanouchi T., Nemoto K., Ohashi M., Kajitani T., and Yamaguchi Y., "The new neutron powder diffractometer with a multi-detector system for high-efficiency and high-resolution measurements" Jpn.J.Appl.Phys. Vol. 37, pp. 3319-3326 (1998).

18. Izumi F. and Ikeda T., "A Rietveld-Analysis Program RIETAN-98 and its Applications to Zeolites" Mater. Sci. Forum Vol. 321-324 pp. 198-203 (2000).

19. Ono Y., Ishikawa R., Miyazaki Y., and Kajitani T., "Neutron diffraction study of layered oxides $Na_x(Co_{1-y}Mn_y)O_{2-}$ " J.Phys.Soc.Jpn. Vol. 70, (Suppl.A), pp. 235-237 (2001).

20. Shannon R. D. and Prewitt C. T., "Effective ionic radii in oxides and fluorides" *Acta Cryst*. B Vol. 25, pp. 925-946 (1969).

21. Kumazawa S., Kubota Y., Takata M., Sakata M., and Ishibashi Y., "MEED: a program packae for electron-density-distribution calculation by the maximum-entropy method" J.Appl.Crystallogr. Vol. 26, pp. 453-457 (1993).